Beneficial effects of citrulline enteral administration on sepsis-induced T cell mitochondrial dysfunction

Florian Reizine[a,b,c], Murielle Grégoire[a,b], Mathieu Lesouhaitier[a,b,c], Valentin Coirier[a,b,c], Juliette Gauthier[a,b], Céline Delaloy[a,b], Elise Dessauge[b], Florent Creusat[b], Fabrice Uhel[a,b,c], Arnaud Gacouin[c,d], Frédéric Dessauge[e], Cécile Le Naoures[f], Caroline Moreau[g], Claude Bendavid[g], Yoann Daniel[h], Kilian Petitjean[h], Valérie Bordeau[i], Claire Lamaison[b], Caroline Piau[j], Vincent Cattoir[i,j,k], Mikael Roussel[a,b], Bernard Fromenty[h], Christian Michelet[c,d], Yves Le Tulzo[c,d], Jaroslaw Zmijewski[l], Ronan Thibault[m,n], Michel Cogné[a,b], Karin Tarte[a,b], and Jean-Marc Tadié[b,c,d,1]

aLaboratoire Suivi Immunologique des Thérapeutiques Innovantes, Centre Hospitalier Universitaire de Rennes, F-35033 Rennes, France; bINSERM, Microenvironment, Cell Differentiation, Immunology, and Cancer–UMR_S1236, Établissement française du sang Bretagne, Université de Rennes 2, F-35000 Rennes, France; cService des Maladies Infectieuses et Réanimation Médicale, Centre Hospitalier Universitaire de Rennes, F-35033 Rennes, France; dINSERM, Centre d'Investigation Clinique de Rennes, Centre Hospitalier Universitaire de Rennes, F-35000 Rennes, France; ePEGASE, INRAE, Institut Agro, 35590 Saint Gilles, France; fLaboratoire d'anatomie pathologie, Centre Hospitalier Universitaire de Rennes, F-35033 Rennes, France; gLaboratoire de Biochimie, Pôle Biologie, Centre Hospitalier Universitaire de Rennes, F-35033 Rennes, France; hUMR_A 1341, UMR_S 1241, INSERM, Institut de Nutrition, Métabolismes et Cancer, Institut National de Recherche Agronomique, Université de Rennes 2, F-35000 Rennes, France; iBACTERIAL REGULATORY RNAS AND MEDICINE–UMR_S 1230, INSERM, Université de Rennes 2, F-35000 Rennes, France; jService de Bactériologie, Centre Hospitalier Universitaire de Rennes, F-35033 Rennes, France; kCentre National de Référence de la Résistance aux Antibiotique (laboratoire associé "Entérocoques"), Centre Hospitalier Universitaire de Rennes, F-35043 Rennes, France; lDepartment of Medicine, University of Alabama at Birmingham, Birmingham, AL 35294; mINSERM, Service d'Endocrinologie, Diabétologie et Nutrition, Institut National de Recherche Agronomoque, Centre Hospitalier Universitaire de Rennes, F-35033 Rennes, France; and nINSERM, Institut de Nutrition, Métabolismes et Cancer, Institut National de Recherche Agronomique, Centre Hospitalier Universitaire de Rennes, F-35000 Rennes, France

Severe sepsis induces a sustained immune dysfunction associated with poor clinical behavior. In particular, lymphopenia along with increased lymphocyte apoptosis and decreased lymphocyte proliferation, enhanced circulating regulatory T cells (Treg), and the emergence of myeloid-derived suppressor cells (MDSCs) have all been associated with persistent organ dysfunction, secondary infections, and late mortality. The mechanisms involved in MDSC-mediated T cell dysfunction during sepsis share some features with those described in malignancies such as arginine deprivation. We hypothesized that increasing arginine availability would restore T cell function and decrease sepsis-induced immunosuppression. Using a mouse model of sepsis based on cecal ligation and puncture and secondary pneumonia triggered by methicillin-resistant *Staphylococcus aureus* inoculation, we demonstrated that citrulline administration was more efficient than arginine in increasing arginine plasma levels and restoring T cell mitochondrial function and proliferation while reducing sepsis-induced Treg and MDSC expansion. Because there is no specific therapeutic strategy to restore immune function after sepsis, we believe that our study provides evidence for developing citrulline-based clinical studies in sepsis.

citrulline | sepsis | mitochondria | T cell

Sepsis is a common cause of morbidity and mortality in intensive care units (ICUs) (1). The initial proinflammatory response associated with sepsis is essential for microbiological clearance and involves the activation of the immune system. However, sepsis induces as well a sustained immune dysfunction, also known as immuno-paralysis or immunosuppression, which has been well characterized over the past years through the functional analysis of immune cells and clinical evidences such as high rates of ICU-acquired infections or the reactivation of latent viruses (2, 3). In particular, lymphopenia along with increased lymphocyte apoptosis and decreased lymphocyte proliferation, enhanced circulating regulatory T cells (Treg), and the emergence of myeloid-derived suppressor cells (MDSC) have all been associated in critically ill septic patients with persistent organ dysfunction such as acute lung injury (ALI), nosocomial infections acquisitions, and poor outcomes (4–6). Although underlying mechanisms in MDSC-associated immunosuppression in severe infection remain to be exhaustively understood,

several data suggest that mechanisms involved in MDSC-mediated T cell dysfunction shared some features with those described in malignancies, including arginase-induced arginine depletion that could be responsible for T cell mitochondrial dysfunction and enhanced apoptosis (7–11). Along these lines, in specific catabolic conditions such as sepsis, de novo arginine synthesis is not sufficient and becomes an essential amino acid. Consequently, sepsis induces an arginine-deficiency state, and arginine deficiency has been associated with an increased incidence of nosocomial infection and mortality (12–15).

Arginine administration in septic patients might thus result in better clinical outcomes. While immune modulating diets containing arginine are conceptually appealing, data from clinical trials and several meta-analyses have failed to produce convincing evidence in sepsis (16). These results have been

Significance

Since sepsis induces a sustained immunosuppression responsible for secondary infections acquisition and late mortality, restoring immune function would result in a better outcome. Given the role of arginine deficiency in T cell dysfunction, the evaluation of restoring arginine availability in sepsis has to be explored. Using an animal model of sepsis, we demonstrated that increasing arginine availability enhanced mitochondrial T cell function and decreased sepsis-induced immunosuppression.

confounded by grouping different formulas and different types of patients together, introducing heterogeneity and perhaps masking treatment effects (17, 18). Furthermore, early enteral administration of arginine in critically ill patients mainly enhanced ornithine synthesis, suggesting a preferential use by the arginase pathway, while nitric oxide synthesis was barely stimulated, and immune functions were unaffected (19). Recently, several studies have found that supplementation with citrulline, which is converted in arginine through the activity of argininosuccinate synthase and argininosuccinate lyase and does not undergo first-pass metabolism, was more efficient than arginine to increase the plasma level of arginine (12).

Using a mouse model of sepsis with secondary infection, we aimed to demonstrate that supplementation with citrulline was more efficient than that with arginine to increase systemic arginine availability. We also analyzed in detail how such supplementation could improve T cell function in blood and spleen and alleviate immunosuppression in postsepsis conditions, notably by increasing T cell mitochondrial function and proliferation.

Results

Cecal Ligation and Puncture Induces Immunosuppression and Arginine Depletion. We first evaluated whether a model of cecal ligation and puncture (CLP) rescued by antibiotic treatment could be relevant to address the question of sepsis-related arginine depletion (Fig. 1*A*). As expected, CLP induced an increase in peripheral blood and spleen T cell apoptosis in vivo and a decrease in T cell capacity to proliferate in vitro in response to stimulation by anti-CD3e/anti-CD28 antibodies, both features classically associated with sepsis-related immune paralysis (Fig. 1 *B–D*). CLP did not impact T cell cycle progression (*SI Appendix*, Fig. S3*A*). Lymphocytes are primarily using mitochondria to meet their energetic demands, and their clonal expansion and optimal activation normally associate with a switch to a metabolic phenotype with increased glycolysis and mitochondrial oxygen consumption rate (OCR). An analysis of peripheral blood CD3^pos T cell mitochondrial mass by flow cytometry using the MitoTracker Green probe did not find any difference between CLP and sham mice. However, T cells isolated 5 d after CLP exhibited a decrease in maximal mitochondrial OCR compared to T cells from sham mice (Fig. 1*E*). An analysis of spleen T cells further confirmed the decrease in maximal mitochondrial OCR and revealed a reduced adenosine triphosphate (ATP) production after CLP (Fig. 1*F*). Moreover, CLP induced an expansion of circulating regulatory T cells and both granulocytic (G-) and myeloid (M-) MDSC at day 5 in the CLP group compared to the sham group (Fig. 1*G*). Importantly, the plasma levels of arginine and citrulline were significantly lower in the CLP group in association with an increased arginase activity evaluated using the arginine-to-ornithine ratio (Fig. 1*H*). Of note, CLP induced a significant decrease of *CD247/CD3 ζ* expression on spleen T cells (*SI Appendix*, Fig. S3*B*). Taken together, these data identify our CLP model as appropriate to evaluate immunological consequences of sepsis-induced arginine depletion.

CLP Induces ALI and Worsens the Secondary Infection. Since sepsis is associated with secondary organ dysfunction, we evaluated whether our CLP-induced sepsis was associated with ALI (Fig. 2*A*). Histological evidence of ALI were found after CLP in mice (Fig. 2*B*). Since the purpose of this study was to develop a clinically relevant "two-hit" model of sepsis that would reflect delayed mortality because of secondary nosocomial infection, we then performed experiments to demonstrate that sepsis worsened the severity of secondary infection in a model of methicillin-resistant *Staphylococcus aureus* (MRSA)-induced pneumonia. Bacterial counts performed 12 h after pneumonia

initiation and determined by quantitative cultures of bronchoalveolar lavages (BAL) were higher in CLP mice compared to sham mice (Fig. 2*C*). Moreover, MRSA systemic dissemination after lung instillation was increased in the CLP group as shown by higher bacterial counts in both spleen and kidneys homogenates (Fig. 2*C*). The pathological examination of lung tissues 12 h after pneumonia initiation found a higher ALI score in CLP mice compared to sham, with extensive cell infiltration and loss of alveolar structure (Fig. 2*D*). As expected, survival rates were lower in mice undergoing CLP compared to sham with a mortality of 20.6% (22/107) within the first 5 d following CLP surgery versus 1.8% (2/109) in sham-operated mice ($P < 0.001$, Fig. 2*E*). Moreover, the mortality related to the secondary pneumonia was also higher in the CLP group compared to the sham group (63.6%, 7/11 versus 0%, 0/12, $P = 0.002$, Fig. 2*F*). These data highlight the higher severity of MRSA-induced pneumonia in mice surviving CLP.

Citrulline Administration after CLP Increases Plasma Arginine and Restores Immune Function. We then explored the consequences of enteral citrulline administration (150 mg/kg/day for 5 d) on CLP-induced immune dysfunction (Fig. 3*A*). Citrulline administration after CLP increased significantly both citrulline and arginine plasma levels compared to placebo or arginine administration, whereas arginase activity was not different between the three groups of mice (Fig. 3*B*). In agreement, the number of Treg was lower in mice receiving citrulline compared to mice receiving arginine or placebo after CLP (Fig. 3*C*). Furthermore, MDSC subset analysis revealed a significant decrease in M-MDSC number in the citrulline group compared to placebo and arginine groups, while there were no differences between the three groups when analyzing G-MDSC (Fig. 3*C*). Citrulline administration induced a significant decrease in T cell apoptotic rate in vivo together with an increase in T cell proliferation index under in vitro activation by anti-CD3e/anti-CD28 antibodies (Fig. 3 *D–F*). Conversely, overcoming arginine deficiency did not restore *CD247/CD3ζ* expression in T cells nor did it affect their capacity to produce nitric oxide after in vitro stimulation (*SI Appendix*, Fig. S3 *B* and *C*). We then evaluated mitochondrial activity in T cells from CLP mice receiving or not receiving arginine or citrulline. Noteworthy, isolated T cells from mice receiving citrulline unlike arginine after CLP had a significantly higher mitochondrial OCR compared to mice receiving the placebo in the absence of the modification of mitochondrial mass (Fig. 3*G*). When analyzing glycolysis activity, citrulline and arginine restored extracellular acidification rate (ECAR) (*SI Appendix*, Fig. S4 *A* and *B*). Citrulline administration also significantly increased ATP production and maximal mitochondrial OCR in spleen T cells (Fig. 3*H*). Of note, improved mitochondrial function was associated with increased expression of oxidative phosphorylation (OXPHOS) complex subunits in spleen T cells (*SI Appendix*, Fig. S4*C*). These data demonstrate that a citrulline-enriched diet efficiently increases the plasma arginine concentration and restores T cell metabolic and proliferative functions after CLP.

Citrulline Administration Decreases CLP-Associated Lung Injury and the Severity of Secondary Infection. Having highlighted the immunological consequences of citrulline administration in septic mice, we next decided to evaluate its clinical impact (Fig. 4*A*). Lung histological examination revealed that CLP-induced ALI was less severe in mice treated with citrulline, unlike arginine, compared to mice receiving placebo (Fig. 4*B*). When MRSA pneumonia was induced at day 5 after CLP, lung injury was more pronounced in mice having received placebo or arginine compared to citrulline (Fig. 4*C*). Additionally, bacteriological cultures of BAL, spleen, and kidney homogenates found a significant decrease in bacterial load in mice receiving the
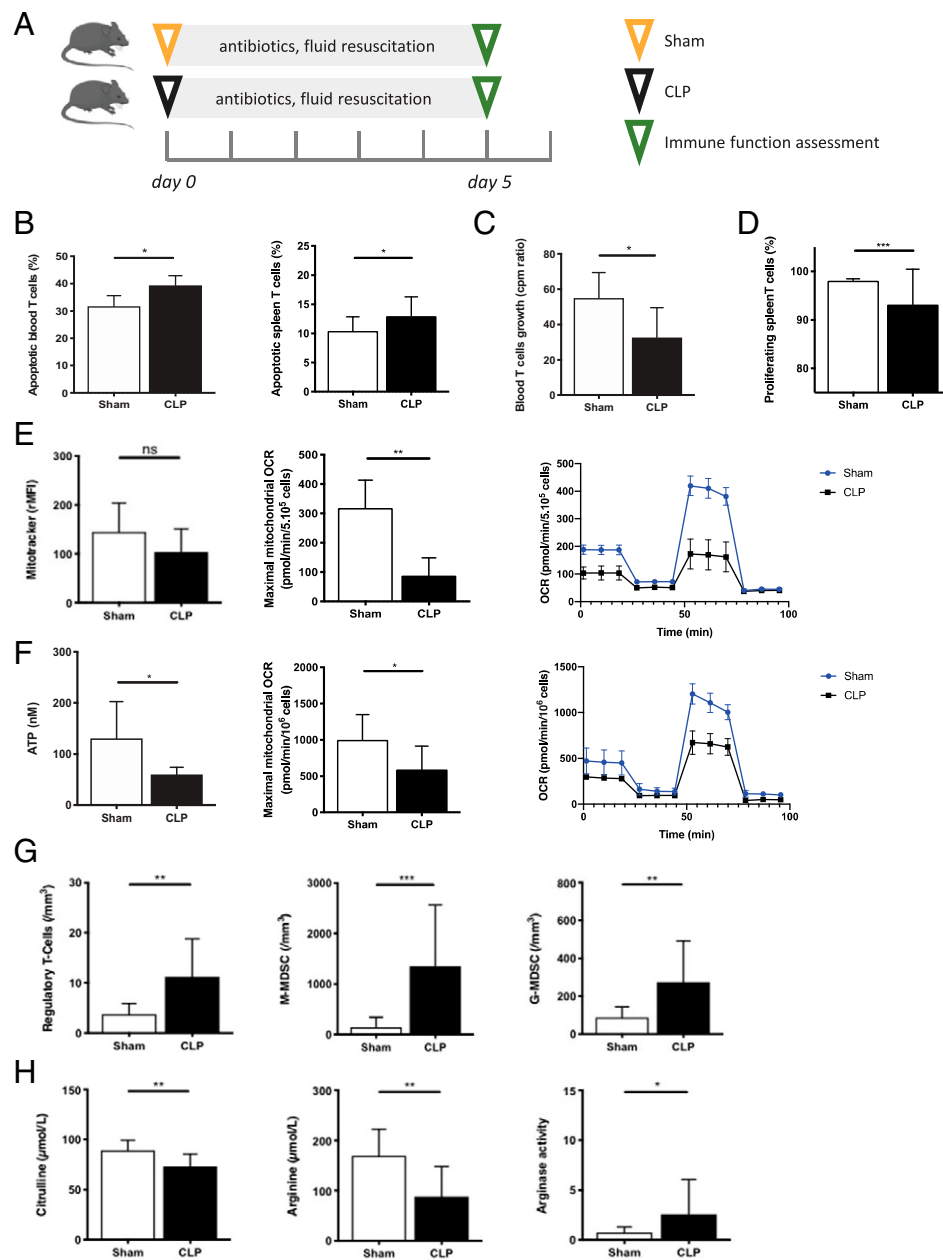
Reizine et al.
Beneficial effects of citrulline enteral administration on sepsis-induced
T cell mitochondrial dysfunction

Fig. 1. The impact of sepsis on immune functions, metabolic disturbances, and mitochondrial properties. (*A*) Animals underwent CLP or sham laparotomy and received antibiotic therapy and fluid resuscitation to create a clinically relevant sepsis model. The immune dysfunction following sepsis was studied 5 d after surgery. (*B*) T cell apoptosis was assessed by flow cytometry as the percentage of AnnexinVpos/DAPIneg CD3pos cells in peripheral blood (*Left*; Sham n = 19; CLP n = 20) and spleen (*Right*, Sham n = 11; CLP n = 11). (*C*) Peripheral blood T cell growth was determined by the incorporation of [3H] thymidine after 48 h of in vitro stimulation by anti-CD3/anti-CD28 antibodies. The data are expressed as the ratios of the counts per minute (cpm) obtained with stimulated versus nonstimulated T cells (Sham n = 19; CLP n = 20). (*D*) Spleen T cell proliferation was determined by CFSE dilution under in vitro stimulation by anti-CD3/anti-CD28 antibodies. The data are expressed as the proportion (%) of proliferative T cells among living T cells (Sham n = 11; CLP n = 11). (*E*) Peripheral blood CD3pos T cell mitochondrial mass was analyzed by flow cytometry using MitoTracker probe (*Left*, Sham n = 20; CLP n = 11) while maximal mitochondrial OCR was determined using Seahorse XF-24 extracellular flux analyzer (*Right*, Sham n = 5; CLP n = 5). (*F*) Spleen CD3pos T cell ATP production (*Left*) and maximal mitochondrial OCR (*Right*) were defined by CellTiter-Glo Luminescent Cell viability assay and Seahorse XF-24 extracellular flux analyzer, respectively (Sham n = 7; CLP n = 7). (*G*) The quantification of Treg (Sham n = 20; CLP n = 13) and monocytic and granulocytic myeloid-derived suppressor cells (M-MDSC and G-MDSC, Sham n = 11; CLP n = 11) by flow cytometry within peripheral blood of CLP versus sham mice. (*H*) Plasmatic amino acid concentrations were assessed by high-performance liquid chromatography (HPLC). Arginase activity was defined by the ornithine-to-arginine ratio (Sham n = 10; CLP n = 14). *$P < 0.05$; **$P < 0.01$; ***$P < 0.001$; ns: nonsignificant.

citrulline-enriched diet compared to placebo, whereas arginine supplementation was not efficient (Fig. 4*D*). However, the beneficial effect of citrulline administration on bacterial clearance was not sufficient by itself for significantly extending the CLP survival rate compared to arginine- or placebo-treated mice (*SI Appendix*, Fig. S4*D*).

Discussion

Our study highlights a promising role for citrulline administration during sepsis to restore immune functions through maintaining plasma arginine levels, preserving T cell mitochondrial function, and decreasing the severity of sepsis-associated lung injury and the severity of secondary infection.
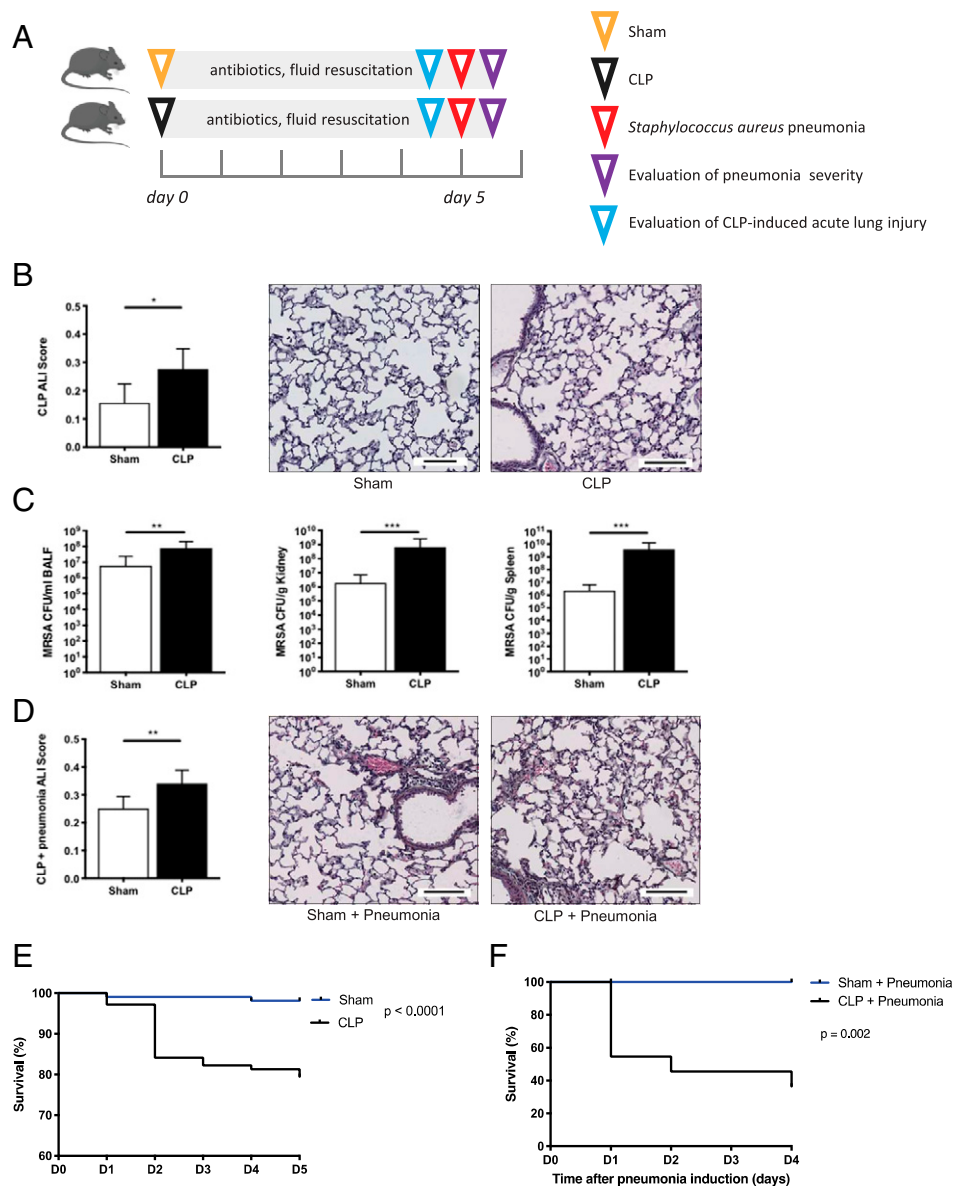
Fig. 2. The impact of CLP on ALI and secondary infection severity. (*A*) Animals underwent CLP or sham laparotomy and received antibiotic therapy and fluid resuscitation to create a clinically relevant sepsis model. Sepsis-induced ALI was evaluated 5 d after surgery. The second set of experiments studied the severity of a secondary infection following sepsis (MRSA-induced pneumonia). The severity of the secondary infection was evaluated 12 h after pneumonia initiation. (*B*) The ALI score was determined by pathological examination of lung tissues 5 d after surgery in CLP and sham mice, and representative images of lung tissues show the differences between sham and septic mice (Sham *n* = 6; CLP *n* = 6). (Scale bar, 100 μm.) (*C*) Bacterial counts were determined 12 h after the tracheal instillation of MRSA in sham and CLP mice by quantitative cultures of BALF (Sham *n* = 12; CLP *n* = 9), spleen, and kidney (Sham *n* = 14; CLP *n* = 10) homogenates for 24 h. (*D*) The ALI score was determined by pathological examination of lung tissues 12 h after MRSA instillation in mice that underwent CLP or sham procedure (Sham *n* = 7; CLP *n* = 7). (Scale bar, 100 μm.) (*E* and *F*) The Kaplan–Meier survival curves of CLP versus sham mice without (*Left*, Sham *n* = 107; CLP = 109) and with secondary pneumonia induction (*Right*, Sham *n* = 12; CLP *n* = 11). *$P < 0.05$; **$P < 0.01$; ***$P < 0.001$; ns: nonsignificant.

Although studies in animal models of sepsis have brought several encouraging results, clinical trials failed to provide any evidence for improved survival in critically ill septic patients. These disappointing results have raised doubts about the clinical relevance of such animal models, and numerous limitations have been emphasized to explain discrepancies between animal and human studies (20). Therefore, we first developed a relevant animal model of sepsis following recently published guidelines and demonstrated that our model induced both immunological and clinical markers that have been associated with immunosuppression, nosocomial infection acquisition, and outcome in septic patients (21, 22).

It is well known that sepsis alters both innate and adaptive immunity that is responsible for a high incidence of acquired infection and persistent organ dysfunction (23, 24). In particular, increased T cell apoptosis, decreased T cell proliferation, and MDSC emergence have all been associated with worse outcomes and nosocomial infections (25, 26). We found in our study an increased proportion of circulating MDSC after sepsis that is among the mechanisms involved in acquired immunosuppression. Although suppressive effects of MDSC on T cells are mainly characterized in the tumor microenvironment, several studies have reported that MDSC also impacts T cell function through arginase-1 activity and arginine deprivation
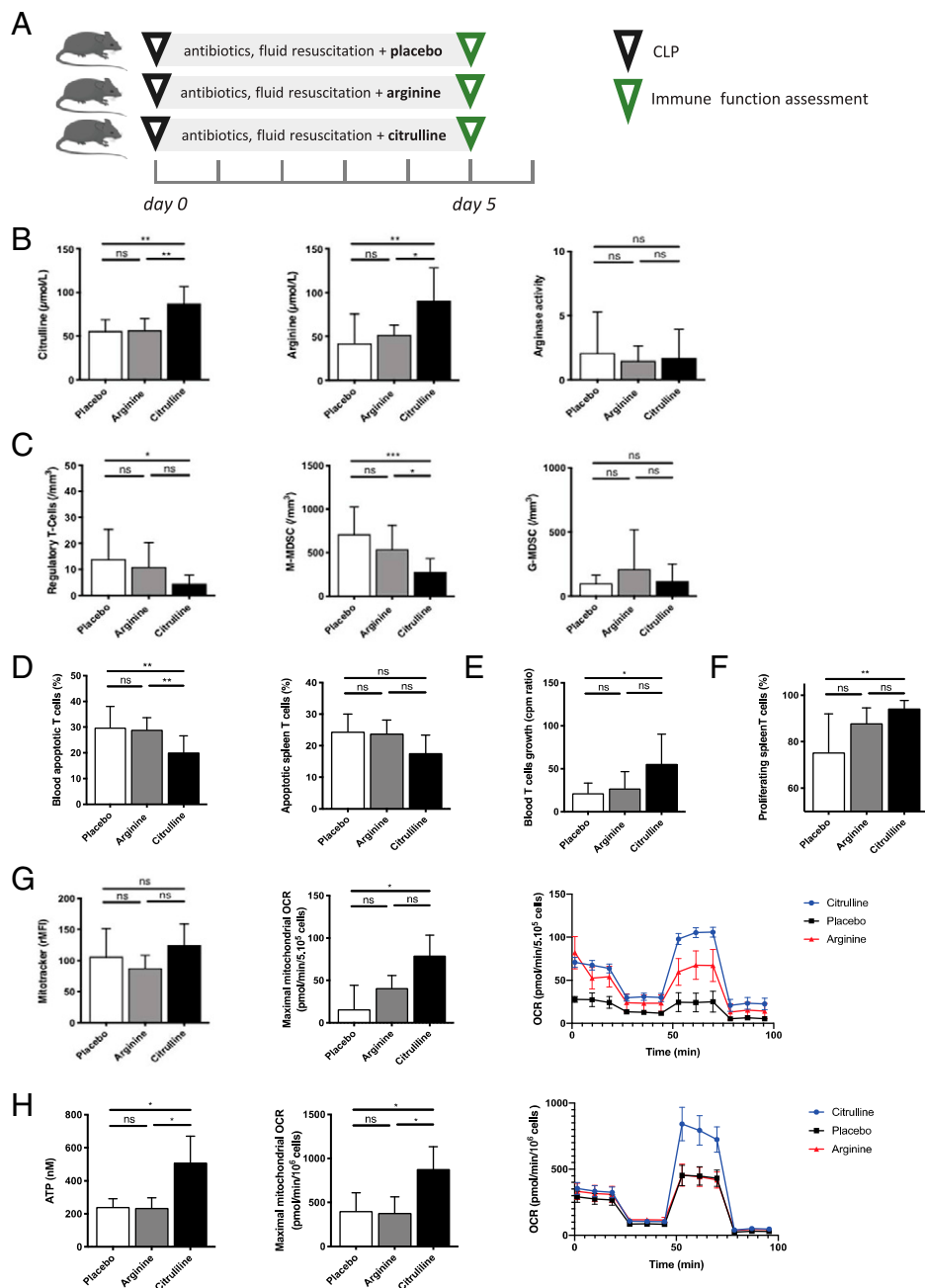
Reizine et al.
Beneficial effects of citrulline enteral administration on sepsis-induced
T cell mitochondrial dysfunction

Fig. 3. The effects of citrulline administration on post-septic immunoparalysis and mitochondrial dysfunctions. (*A*) The animals underwent CLP and received antibiotic therapy and fluid resuscitation. From day 0 to 5, the mice were enterally fed by citrulline (150 mg/kg/day), arginine (150 mg/kg/day), or an isonitrogenous placebo. The immune dysfunctions were studied 5 d after surgery. (*B*) Plasmatic amino acid concentrations were assessed by HPLC. Arginase activity was defined by the ornithine-to-arginine ratio (Sham $n = 10$; CLP $n = 14$) (Placebo $n = 10$, Arginine $n = 13$, and Citrulline $n = 13$). (*C*) The quantification of Treg and M-MDSC and G-MDSC by flow cytometry within peripheral blood of CLP mice (Placebo $n = 14$, Arginine $n = 12$, and Citrulline $n = 14$). (*D*) T cell apoptosis was assessed by flow cytometry as the percentage of AnnexinVpos/DAPIneg CD3pos cells in peripheral blood (Placebo $n = 15$, Arginine $n = 15$, and Citrulline $n = 15$) and spleen (Placebo $n = 8$, Arginine $n = 8$, and Citrulline $n = 8$) of CLP mice. (*E*) Peripheral blood T cell growth was determined by the incorporation of [3H] thymidine after 48 h of in vitro stimulation by anti-CD3/anti-CD28 antibodies. The data are expressed as the ratios of the counts per minute (cpm) obtained with stimulated versus nonstimulated T cells (Placebo $n = 6$, Arginine $n = 7$, and Citrulline $n = 12$). (*F*) Spleen T cell proliferation was determined by CFSE dilution under in vitro stimulation by anti-CD3/anti-CD28 antibodies. The data are expressed as the proportion (%) of proliferative T cells among living T cells. (Placebo $n = 8$, Arginine $n = 8$, and Citrulline $n = 8$). (*G*) Peripheral blood CD3pos T cell mitochondrial mass was analyzed by flow cytometry using MitoTracker probe (*Left*, Placebo $n = 7$, Arginine $n = 4$, and Citrulline $n = 8$), while maximal mitochondrial OCR was determined using Seahorse XF-24 extracellular flux analyzer (*Right*, Placebo $n = 4$, Arginine $n = 4$, and Citrulline $n = 4$). (*H*) Spleen CD3pos T cell ATP production (*Left*) and maximal mitochondrial OCR (*Right*) were defined by CellTiter-Glo Luminescent Cell viability assay and Seahorse XF-24 extracellular flux analyzer, respectively (Placebo $n = 7$, Arginine $n = 7$, and Citrulline $n = 7$). *$P < 0.05$; **$P < 0.01$; ***$P < 0.001$; ns: nonsignificant.

in critically ill patients (8, 9, 27). MDSC comprises a heterogeneous population of immature myeloid cells. Two subsets have been described which are both released from the bone marrow and suppress both adaptive and innate immunity. Although mechanisms responsible for MDSC-mediated immunosuppression in sepsis remain to be exhaustively described,

Reizine et al.
Beneficial effects of citrulline enteral administration on sepsis-induced
T cell mitochondrial dysfunction

PNAS | 5 of 9
https://doi.org/10.1073/pnas.2115139119

Fig. 4. Citrulline mediated ALI's protection and improvement in secondary infection severity. (*A*) The animals underwent CLP or sham laparotomy and received antibiotic therapy and fluid resuscitation to create a clinically relevant sepsis model. From day 0 to 5, the mice were enterally fed by citrulline (150 mg/kg/day), arginine (150 mg/kg/day), or an isonitrogenous placebo. Sepsis-induced ALI was evaluated 5 d after surgery. The second set of experiments studied the severity of a secondary infection following sepsis (MRSA-induced pneumonia). The severity of the secondary infection was evaluated 12 h after pneumonia initiation. (*B*) The ALI score determined by pathological examination of lung tissues 5 d after CLP, and representative images of lung tissues show the differences between the three groups of mice (Placebo $n = 9$, Arginine $n = 7$, and Citrulline $n = 9$) (Sham $n = 6$; CLP $n = 6$). (Scale bar, 100 μm.) The ALI scores were higher in placebo and arginine mice than in citrulline mice. (*C*) Bacterial counts were determined 12 h after the instillation of MRSA in mice by quantitative cultures of BALF, spleen, and kidney homogenates at 24 h was performed. Bacteriological secondary pneumonia severity assessment showed lower MRSA concentrations in BALF (Placebo $n = 8$, Arginine $n = 13$, and Citrulline $n = 13$), spleen, and kidneys (Placebo $n = 15$, Arginine $n = 21$, and Citrulline $n = 20$) of citrulline-fed mice. (*D*) The ALI score was determined by the pathological examination of lung tissues 12 h after the secondary infection initiation, and representative images of lung tissues show the differences between the three groups of mice (Placebo $n = 7$, Arginine $n = 8$, and Citrulline $n = 10$). (Scale bar, 100 μm.) The ALI scores were higher in placebo and arginine mice than in citrulline mice. *$P < 0.05$, ***$P < 0.001$; ns, nonsignificant.

MDSC-induced arginine depletion through arginase-1 activity has been clearly identified in septic patients. For instance, Uhel et al. found that MDSCs producing arginase-1 were associated with higher mortality and higher incidence of nosocomial infections in patients admitted for septic shock. Additionally, the authors found that the depletion of MDSCs completely abrogated arginase-1 activity and increased both CD4^{pos} and CD8^{pos} T cell proliferation (28).

Arginase converts L-arginine to L-ornithine and urea. In normal conditions, arginine is synthesized de novo and therefore not diet dependent (29, 30). However, enhanced arginase activity during critically ill states is responsible for a significant decrease in arginine availability that becomes essential once endogenous arginine synthesis is exceeded (12). This arginine deficiency strongly contributes to T cell dysfunction. The effects of L-arginine starvation in regulating cell cycle in T cells have

been studied, and growing evidence shows that amino acid availability by tumor cells producing arginase is a mechanism by which tumor cells escape immune response (10, 31). Although the role for arginine metabolism in regulating T cell persistence and survival has been studied in T cell antitumor function, several reports have demonstrated the impact of arginine administration in T cell proliferation during active infection such as severe Covid-19. In sepsis, similar interactions have been found between myeloid cells and T cells with an important impact on the patient's outcome (27, 28, 32).

The shortage of L-arginine inhibits T cell proliferation through several mechanisms such as decreasing the expression of CD3 ζ-chain or inducing blockage in cell cycle progression (33). Furthermore, Geiger et al., using proteomics, metabolomics, and functional approaches, have found that increasing the usage of mitochondrial oxidative metabolism promotes T cell

Reizine et al.
Beneficial effects of citrulline enteral administration on sepsis-induced
T cell mitochondrial dysfunction

responses against pathogens (10, 34). Conversely, decreasing L-arginine availability induced a drop in intracellular L-arginine along with altered mitochondrial function highlighted by the significant decrease in the OCR (10). We showed in this study that increasing arginine availability was associated with increased mitochondrial oxidative phosphorylation on the basis of the OCR, along with enhanced proliferation and decreased T cells apoptosis, although we failed to increase the expression of the CD3 ζ-chain. As several studies have shown that mitochondrial energy generation determined the survival and the effectiveness of T cells, our findings are of importance since T cell proliferation inhibition has been associated with worse outcomes in septic shock, and apoptotic cells induce immunosuppression (35). Interestingly, L-arginine starvation could be responsible for T cell proliferation inhibition by inducing the accumulation of MDSCs (29). For instance, Fletcher et al. found that L-arginine deprivation induced the accumulation of MDSCs, which inhibited T cell proliferation in mice (36). These observations are in line with the effect of increasing plasma arginine on the reduction of the circulating M-MDSCs observed in our model. Interestingly, Fletcher et al. also found that de novo synthesis of L-arginine occurs from L-citrulline. In a second step, they compared the efficiency of L-citrulline versus L-arginine supplementation to relieve the proliferation arrest induced by increased arginase-1 activity and found that only L-citrulline restored the proliferation of T cells cultured in the presence of arginase-1.

In humans, it has been demonstrated that L-arginine administration in critically ill patients does not improve immune functions. Conversely, it has been suggested that immunonutrition could be deleterious. These results have been confounded by grouping different formulas and different types of patients together. However, in selected patients such as such as patients undergoing surgery, immune enhancing diets are beneficial, and specific critically ill patients may benefit from the supplementation of individual immunomodulating nutrients (16, 37). In a previous study, we demonstrated that critically ill states were associated with arginine deficiency and that early enteral administration of L-arginine increased ornithine synthesis, suggesting preferential use by the arginase pathway (19). Citrulline is an amino acid that could be transformed into arginine by the arginine–succinate synthase, and several studies have shown that citrulline supplementation served as an arginine precursor more productively than arginine itself in catabolic situations such as sepsis for several reasons (38). Among those, citrulline is not subject to first-pass metabolism, whereas arginine is largely extracted in the liver, and arginine–succinate synthase colocalizes with nitric oxide synthase (29, 39). Accordingly, in our study, citrulline administration increased arginine plasma levels in septic mice, while arginine did not. Noteworthy, the enteral administration of higher doses of arginine or citrulline such as 300 mg/kg has been found to induce adverse gastrointestinal effects without a significant increase in arginine plasma concentration (40, 41). Since plasma citrulline concentration is the primary factor which determines arginine production by the kidneys, the authors suspected that arginine synthesis was probably saturated when using a high dose of citrulline.

Furthermore, we found that Treg were significantly decreased upon the administration of citrulline. Treg suppress responses of other effector T cell subsets and have been associated with mortality in sepsis. Our results are in accordance with the demonstrated effects of arginine depletion in boosting Treg in vitro as well as in vivo since the depletion of arginine in vitro cell cultures stimulates Treg generation which are unaffected by the arginine-deficiency state (42, 43). Along these lines, Treg metabolism has been shown to be more resistant to sepsis-induced apoptosis. Interestingly, as we found a significant decrease in Treg and M-MDSC in the citrulline-treated group, our findings emphasized the crosstalk between these two types of cells, as it

has been demonstrated that M-MDSCs support the expansion of Treg while Treg modulate M-MDSC differentiation and function (44).

Lastly, we found that citrulline administration could diminish CLP-induced ALI. Sepsis is the leading cause of acute respiratory distress syndrome (ARDS) and accounts for up to 30% of the etiology of ARDS. The crucial role of T cells, mainly CD4^{pos}, to decrease both neutrophils lung infiltration and lung cell apoptosis, two mechanisms that contribute to the development of sepsis-associated lung injury, has been highlighted (45). Furthermore, a strong association between low citrulline levels and the presence of ARDS in sepsis patients suggests that nitric oxide synthase (NOS) substrate deficiency might play a role in the pathogenesis of ARDS (46). Therefore, limiting T cell apoptosis and increasing NOS substrate could be responsible for limiting lung injury after sepsis.

While there is no specific therapeutic strategy to restore or preserve immune function in patients with sepsis and alleviate the risk of acquired infection, we believe that our study provides encouraging evidence to study in detail the potential therapeutic interest of nutrients that impact arginine availability in sepsis. Although results from animal studies should be cautiously translated to humans, the next step should be a clinical trial evaluating the immunologic and clinical impacts of citrulline administration in critically ill septic patients without preexisting immunosuppression.

Materials and Methods

Ethic Statement. All the experiments were approved by the Institutional Animal Care and Use Committee of Rennes and by the French Ministry of Education and Research in accordance with the European Convention for the Protection of Vertebrate Animals used for Experimental and other Scientific Purposes (Approval Autorisation de Projet Utilisant des Animaux à des Fins Scientifiques No. 9746–2017042717414943).

Study Design. The first step of our study was to characterize our model of sepsis-induced immunosuppression following recently published recommendations (47–49). For that purpose, we first performed experiments in mice to illustrate sepsis-associated immunosuppression and CLP-induced ALI (Figs. 1A and 2A). Since the purpose of this study was to develop a clinically relevant "two-hit" model of sepsis that would reflect delayed mortality because of secondary nosocomial infection, we then performed experiments to demonstrate that sepsis worsens the severity of secondary infection through a model of MRSA-induced pneumonia (Fig. 2A). Then, we aimed to study the effect of arginine or citrulline enteral administration (150 mg/kg) compared to isonitrogenous placebo on sepsis-induced immunosuppression and the severity of secondary infection (Figs. 3A and 4A, respectively).

Recommendations guided CLP-induced sepsis. Animals (C57BL/6J mice [10-wk-old females] purchased from Janvier Labs) underwent CLP or sham laparotomy as already reported (50). In brief, after buprenorphine subcutaneous injection (100 µg/kg), a midline abdominal incision was made in animals under isoflurane anesthesia. In animals that underwent CLP, the cecum was exposed and ligated in the middle, below the ileocecal valve and punctured once with a 21-gauge needle. A small amount of fecal material was squeezed out of the cecum to induce polymicrobial peritonitis. The cecum was then returned to the abdominal cavity, and the abdominal wall was closed in layers. Antibiotic therapy (25 mg/kg meropenem) was initiated 6 h after CLP or sham surgery and administered by intraperitoneal injection every 24 h for 5 d. Saline for fluid resuscitation was administered to create a more clinically relevant sepsis model, as this is standard care for humans. Buprenorphine for pain relief [based on mouse grimace scale score (51)] was administered within 6 h after CLP. The mice were monitored twice daily to ensure that animal welfare was preserved.

ALI. Histological analysis was performed to assess the occurrence of sepsis-induced ALI. The lungs were harvested 5 d after CLP and fixed with 4% paraformaldehyde (PFA) to perform histologic analysis after hematoxylin and eosin staining. Measurements of histological evidence of ALI (ALI score, *SI Appendix*, Fig. S1A) were performed by a pathologist blinded of mice condition. The histological evidence of ALI was as follows: the accumulation of neutrophils in the alveolar or the interstitial space, the formation of hyaline membranes, the presence of proteinaceous debris in the alveolar space (such as fibrin strands), the thickening of the alveolar wall, and evidence of hemorrhage (52).

Post-sepsis Immune Dysfunction.

Immune parameters. Post-septic immunoparalysis was first assessed by performing biological analysis on the spleen obtained after euthanasia or whole blood that was obtained by direct cardiac puncture under deep anesthesia and placed in a sterile heparinized tube at day 5 after CLP or sham surgery.

Flow cytometry. The quantification of cellular populations was performed on whole blood by using the following antibodies: CD25 (3C7), Ly6G (1A8), CD19 (1D3), CD335 (NKp46), Ter119 (TER-119), CD41 (MWReg30), CD11b (M1/70), CD11c (HL3), Ly6C (AL-21), CD3e (145-2C11), and CD127 (SB/199) (Becton Dickinson). Erythrocytes were then lysed using Easylyse (Dako). The cells were labeled with Di Aminido Phenyl Indol (DAPI) (Sigma-Aldrich) to exclude dead cells, and precision count beads (BioLegend) were added after staining to calculate the absolute number of cell subpopulations. Gating strategies are displayed in *SI Appendix*, Fig. S2. A Fortessa ×20 flow cytometer (Becton Dickinson) was used to run all samples. The data were analyzed using Kaluza 2.0 software.

Peripheral blood T Cell growth. Peripheral blood mononuclear cells (PBMC) were isolated by centrifugation using Ficoll (Eurobio) density gradient. The quantification of T cells was obtained by staining PBMC with a CD3e (145-2C11) antibody (Becton Dickinson). A 96-well round-bottom plate was pre-coated with an anti-CD3e (145-2C11, 5 μg/mL, eBioscience) for 2 h at 37 °C. T cells (2.10^4 cells/well) were added and incubated for 48 h with an anti-CD28 antibody (37.51, 2.5 μg/mL, eBioscience) or complete media for control well in a humidified environment with 5% CO_2 at 37 °C. Then, [3H] thymidine was added in the culture medium (1 μCi/well, PerkinElmer) 16 h before harvesting cells on a fiberglass filter using an automated cell harvester (PerkinElmer). Incorporated radioactivity was measured in a direct beta counter (Top Count, PerkinElmer). The results were expressed as a proliferation ratio between counts per minute measured in stimulated and nonstimulated wells for the same sample.

Splenocyte T cell proliferation. The splenocytes were isolated, mashing spleen with a plunger end of syringe into a 40-μm cell strainer. The erythrocytes were lysed using Easylyse (Dako). The cells were then labeled with 0.2 μM carboxyfluorescein succinimidyl ester (CFSE; Intercom). A 96-well round-bottom plate was precoated with an anti-CD3e (145-2C11, 5 μg/mL, eBioscience) for 2 h at 37 °C. The T cells (10^5 cells/well) were added and incubated for 72 h with an anti-CD28 antibody (37.51, 2.5 μg/mL, eBioscience) or complete media for control well in a humidified environment with 5% CO_2 at 37 °C. After 3 d of culture, the cells were harvested and labeled with CD4 (GK1.5), CD8 (53-6.7) antibodies (BD Biosciences), and FVS780 (BD Biosciences) for cell viability. CFSE dilution was assessed by flow cytometry on a Fortessa X-20, and results were analyzed with ModFit LT software.

Amino acid quantification. Citrulline, arginine, and ornithine concentrations were determined by ion-exchange chromatography. Arginase activity was evaluated by measuring the ratio between arginine and ornithine concentrations.

Apoptotic analysis. To evaluate the proportion of apoptotic T cells, whole blood or splenocytes were incubated with CD3e (145-2C11), CD4 (GK1.5), and CD8 (53-6.7) antibodies (Becton Dickinson). The cells were then stained with fluorescein isothiocyanate annexinV (Tau Technologies) and DAPI (Sigma-Aldrich). AnnexinV^{pos}/DAPI^{neg} cells were considered apoptotic.

Mitochondrial Analysis.

Mitochondrial mass. Whole blood was first labeled with a CD3e (145-2C11) antibody, and the erythrocytes were then lysed using Easylyse (Dako). The quantification of mitochondrial mass into T cells was performed using the MitoTracker Green probe (Invitrogen). The cells were incubated for 20 min at 37 °C before washing in phosphate-buffered saline (PBS) and running in a Fortessa ×20 flow cytometer (Becton Dickinson).

Mitochondrial function. OCR and ECAR were measured using the Seahorse XF-24 extracellular flux analyzer (Seahorse Bioscience). For peripheral T cells, OCR was analyzed after 4 d of PBMC culture into complete media and stimulated with anti CD3e/anti CD28. T cells were purified using Pan T Cell Isolation Kit II (Miltenyi). The cells were pooled, counted, and 5.10^5 cells per well were plated in Seahorse XFe24 cell culture plate (Agilent Technologies) pretreated with poly L-lysine. For spleen T cells, T cells were purified from splenocytes using the Pan T Cell Isolation Kit II (Miltenyi) and were seeded at 10^6 per well. The T cells were incubated for 45 min in a CO_2-free incubator in Seahorse XF Dulbecco's modified Eagle's medium (Agilent Technologies) supplemented with glucose (10 mM, Sigma-Aldrich), sodium pyruvate (1 mM, Life Technologies), and glutamine (2 mM, Life Technologies). Mitochondrial respiration was performed using a Seahorse XF-24 extracellular flux analyzer and the Seahorse XF Cell Mito Stress Test Kit (Agilent Technologies). The cells were treated with oligomycin (2 μM), carbonyl cyanide 4-(trifluoromethoxy)phenylhydrazone (2 μM), and Rotenone/Antimycin A (2 μM) at indicated time points.

ATP measurement. Intracellular ATP content was measured using CellTiter-Glo Luminescent Cell viability assay (Promega). Briefly, cells (5.10^4) were incubated with the CellTiter-Glo reagent for 10 min. Lysate was transferred to an opaque multi-well plate, and luminescent signal was quantified at 540 nm using the Polarstar Omega microplate reader (BMG Labtech). ATP content was calculated using an ATP standard curve.

Cell cycle. The mice were injected with 20 mg 5-ethynyl-2′-deoxyuridine (EdU) (Invitrogen) 24 h before euthanasia. The spleens were harvested, perfused with Roswell Park Memorial Institute medium fetal bovine serum-10%, and filtered at 70 μm. The erythrocytes were lysed using Easylyse (Dako), and the cells were washed in PBS BSA-1%. A total of 0.5×10^6 cells were incubated with CD3e antibody (145-2C11, Becton Dickinson) for 20 min at 4 °C. The cells were washed in PBS bovine serum albumin-1% (BSA-1%) and fixed for 15 min at room temperature with Click-iT fixative (Click-iT Plus EdU Flow Cytometry Assay Kit, Life Technologies). The cells were washed in PBS BSA-1% and incubated with Click-iT saponin-based permeabilization and wash reagent and Click-iT Plus reaction mixture for 30 min at room temperature. The cells were washed with Click-iT saponin-based permeabilization and wash reagent. The cells were resuspended in Click-iT saponin-based permeabilization and wash reagent with Dapi at 10 μg/mL and incubated for 20 min at room temperature before running the sample in a Fortessa ×20 flow cytometer.

Real-time qPCR. RNA was generated from splenocytes (Macherey–Nagel). Complementary deoxyribonucleic acid synthesis was performed with the SuperScript II reverse transcriptase and random primers (Thermo Fisher Scientific). For qRT-PCR, we used assay-on-demand primers and probes and Taqman Universal Master Mix (Thermo Fisher Scientific). Gene expression was measured using the StepOnePlus based on the ΔCt calculation method. *B2M* was used as endogenous control (Mm00437762_m1, Thermo Fisher Scientific). For each sample, relative expression to *B2M* were determined for *CD3z* (Mm00446171_m1) and *CD3e* (Mm01179194_m1). The results are then presented as a ratio between *CD3z* and *CD3e* expression levels in order to normalize for CD3 cell frequency between the samples.

NO measurement. To determine the NO concentration, the culture supernatant from PBMC stimulated by anti-CD3/anti-CD28 antibodies for 4 d was collected and centrifuged at 1,500 × *g* for 10 min and conserved at −20 °C until use. According to the manufacturer's instructions, supernatants were quantified for nitrates by using the nitric oxide assay kit (Thermo Fisher Scientific).

Western blot analysis. The proteins were extracted from pelleted T cells using the radioimmunoprecipitation assay extraction reagent (Fisher Scientific). The soluble protein fraction was collected after centrifugation at 14,000 × *g* for 20 min (4 °C), and protein concentrations were determined using the bicinchoninic acid Protein Assay Kit (Fisher Scientific) according to the manufacturer's instructions. The lysates were combined with sample buffer (50 mM Tris HCl [pH 6.8], 2% sodium dodecyl sulfate (SDS), 0.1% bromophenol blue, 20% glycerol, and 0.1 M dithiothreitol), and resolved using SDS-PAGE. Equal amounts of protein (10 μg) were separated on 4 to 12% NuPage gradient gels (Fisher Scientific) via SDS-PAGE (polyacrylamide gel electrophoresis) and transferred electrophoretically to polyvinylidene difluoride membranes (Amersham) in N-cyclohexyl-3-aminopropanesulfonic acid buffer (Fisher Scientific) at 100 V for 90 min. A set of prestained molecular mass standards (protein ladder) was run into each gel. The membranes were incubated with blocking solution (5% blotting grade blocker; Bio-Rad) dissolved in Tris-buffered saline-Tween buffer (50 mM Tris HCl [pH 8.6], 150 mM NaCl, and 0.1% Tween) for 60 min. These membranes were incubated overnight at 4 °C with primary antibodies: Total OXPHOS Rodent Western Blot Antibody Mixture (ab110413, Abcam) and β-actin (A5441, Sigma). They were also incubated with the appropriate secondary antibody coupled to horseradish peroxidase used at 1:2,500. The horseradish peroxidase chemiluminescence was visualized using an enhanced chemiluminescence kit and the ImageQuant LAS4000 Biomolecular Imager digital imaging system (GE Healthcare). The images generated as gel files were analyzed using the corresponding ImageQuant TL software (GE Healthcare).

Secondary Infection Following CLP-induced Sepsis.

The surviving mice were anesthetized with isoflurane and held vertically by holding their upper incisor teeth 5 d after CLP or sham surgery. The tongue was gently extended, and a solution of 50 μL containing 5.10^7 colony forming unit MRSA strain (National Collection of Type Cultures 12493) was slowly delivered above the trachea. MRSA was selected because it is a gram-positive bacterium resistant to meropenem that is commonly responsible for nosocomial pneumonia that mainly occurs within the first week of hospitalization (53).

Bacterial dissemination. The mice were sacrificed by CO_2 inhalation 12 h after the induction of pneumonia. BAL was performed, as already reported, by cannulating the trachea and lavaging the lungs with 1 mL sterile saline, about 800 μL BAL fluid was recovered from each mouse (54). The spleen and kidneys were harvested by sterile technique, weighed, and homogenized with a sterile tissue grinder (Ultrathurax). Viable bacterial counts were determined in bronchoalveolar lavage fluid (BALF), kidneys, and spleen after being seeded on tryptic soy agar plates (Oxoid) and incubated at 35 °C under aerobic conditions. MRSA colonies were counted after 24 h incubation. Growth was calculated as colony-forming units/mL for BAL or as colony-forming units/g for kidneys and spleen. The severity of pneumonia was quantified using ALI score of lungs fixed with PFA 4% and harvested to perform a histologic analysis of hematoxylin and eosin stained lung specimens (52). A survival study of mice within 4 d following pneumonia initiation was performed.

Statistical Analysis. All data were analyzed with GraphPad Prism 9. Differences among groups in flow cytometric analyses were evaluated by Mann–Whitney *U* or Kruskal–Wallis tests as appropriate. The log-rank test was used for comparing survival data. *P* values < 0.05 were considered statistically significant.

Data Availability. All study data are included in the article and/or *SI Appendix*.

1. D. C. Angus, T. van der Poll, Severe sepsis and septic shock. *N. Engl. J. Med.* **369**, 840–851 (2013).
2. M. J. Delano, P. A. Ward, Sepsis-induced immune dysfunction: Can immune therapies reduce mortality? *J. Clin. Invest.* **126**, 23–31 (2016).
3. C. F. Benjamim, C. M. Hogaboam, S. L. Kunkel, The chronic consequences of severe sepsis. *J. Leukoc. Biol.* **75**, 408–412 (2004).
4. F. Daviaud *et al.*, Timing and causes of ARDS in septic shock. *Ann. Intensive Care* **5**, 16 (2015).
5. F. Venet, G. Monneret, Advances in the understanding and treatment of sepsis-induced immunosuppression. *Nat. Rev. Nephrol.* **14**, 121–137 (2018).
6. J. S. Boomer *et al.*, Immunosuppression in patients who die of sepsis and multiple organ failure. *JAMA* **306**, 2594–2605 (2011).
7. D. I. Gabrilovich, S. Nagaraj, Myeloid-derived suppressor cells as regulators of the immune system. *Nat. Rev. Immunol.* **9**, 162–174 (2009).
8. F. Veglia, M. Perego, D. Gabrilovich, Myeloid-derived suppressor cells coming of age. *Nat. Immunol.* **19**, 108–119 (2018).
9. E. J. Wherry, T cell exhaustion. *Nat. Immunol.* **12**, 492–499 (2011).
10. R. Geiger *et al.*, L-Arginine modulates T cell metabolism and enhances survival and anti-tumor activity. *Cell* **167**, 829–842.e13 (2016).
11. P. Raber, A. C. Ochoa, P. C. Rodríguez, Metabolism of L-arginine by myeloid-derived suppressor cells in cancer: Mechanisms of T cell suppression and therapeutic perspectives. *Immunol. Invest.* **41**, 614–634 (2012).
12. K. A. Wijnands, T. M. Castermans, M. P. Hommen, D. M. Meesters, M. Poeze, Arginine and citrulline and the immune response in sepsis. *Nutrients* **7**, 1426–1463 (2015).
13. J. M. Tadié *et al.*, Prediction of nosocomial infection acquisition in ventilated patients by nasal nitric oxide: Proof-of-concept study. *Shock* **34**, 217–221 (2010).
14. V. Bronte, P. Zanovello, Regulation of immune responses by L-arginine metabolism. *Nat. Rev. Immunol.* **5**, 641–654 (2005).
15. A. Gey *et al.*, Granulocytic myeloid-derived suppressor cells inversely correlate with plasma arginine and overall survival in critically ill patients. *Clin. Exp. Immunol.* **180**, 280–288 (2015).
16. T. W. Rice, Immunonutrition in critical illness: Limited benefit, potential harm. *JAMA* **312**, 490–491 (2014).
17. A. R. van Zanten *et al.*, High-protein enteral nutrition enriched with immune-modulating nutrients vs standard high-protein enteral nutrition and nosocomial infections in the ICU: A randomized clinical trial. *JAMA* **312**, 514–524 (2014).
18. G. Bertolini *et al.*, Early enteral immunonutrition in patients with severe sepsis: Results of an interim analysis of a randomized multicentre clinical trial. *Intensive Care Med.* **29**, 834–840 (2003).
19. J. M. Tadié *et al.*, Arginine administration to critically ill patients with a low nitric oxide fraction in the airways: A pilot study. *Intensive Care Med.* **39**, 1663–1665 (2013).
20. M. Bara, A. R. Joffe, The methodological quality of animal research in critical care: The public face of science. *Ann. Intensive Care* **4**, 26 (2014).
21. M. F. Osuchowski *et al.*, Minimum quality threshold in pre-clinical sepsis studies (MQTiPSS): An international expert consensus initiative for improvement of animal modeling in sepsis. *Shock* **50**, 377–380 (2018).
22. C. S. Deutschman, Translational research: The model matters. *Crit. Care Med.* **46**, 835–837 (2018).
23. J. C. Mira *et al.*, Sepsis pathophysiology, chronic critical illness, and persistent inflammation-immunosuppression and catabolism syndrome. *Crit. Care Med.* **45**, 253–262 (2017).
24. F. Pène, P. Pickkers, R. S. Hotchkiss, Is this critically ill patient immunocompromised? *Intensive Care Med.* **42**, 1051–1054 (2016).
25. Y. Le Tulzo *et al.*, Early circulating lymphocyte apoptosis in human septic shock is associated with poor outcome. *Shock* **18**, 487–494 (2002).
26. C. Cao, M. Yu, Y. Chai, Pathological alteration and therapeutic implications of sepsis-induced immune cell apoptosis. *Cell Death Dis.* **10**, 782 (2019).
27. F. Reizine *et al.*, SARS-CoV-2-induced ARDS associates with MDSC expansion, lymphocyte dysfunction, and arginine shortage. *J. Clin. Immunol.* **41**, 515–525 (2021).
28. F. Uhel *et al.*, Early expansion of circulating granulocytic myeloid-derived suppressor cells predicts development of nosocomial infections in patients with sepsis. *Am. J. Respir. Crit. Care Med.* **196**, 315–327 (2017).
29. R. W. Caldwell, P. C. Rodriguez, H. A. Toque, S. P. Narayanan, R. B. Caldwell, Arginase: A multifaceted enzyme important in health and disease. *Physiol. Rev.* **98**, 641–665 (2018).
30. S. M. Morris Jr., Arginine metabolism revisited. *J. Nutr.* **146**, 2579S–2586S (2016).
31. D. S. Thommen, T. N. Schumacher, T cell dysfunction in cancer. *Cancer Cell* **33**, 547–562 (2018).
32. X. Zhu *et al.*, The central role of arginine catabolism in T-cell dysfunction and increased susceptibility to infection after physical injury. *Ann. Surg.* **259**, 171–178 (2014).
33. P. C. Rodriguez, D. G. Quiceno, A. C. Ochoa, L-arginine availability regulates T-lymphocyte cell-cycle progression. *Blood* **109**, 1568–1573 (2007).
34. E. L. Mills, B. Kelly, L. A. J. O'Neill, Mitochondria are the powerhouses of immunity. *Nat. Immunol.* **18**, 488–498 (2017).
35. C. Guignant *et al.*, Programmed death-1 levels correlate with increased mortality, nosocomial infection and immune dysfunctions in septic shock patients. *Crit. Care* **15**, R99 (2011).
36. L. Fletcher *et al.*, l-Arginine depletion blunts antitumor T-cell responses by inducing myeloid-derived suppressor cells. *Cancer Res.* **75**, 275–283 (2015).
37. R. Tepaske *et al.*, Effect of preoperative oral immune-enhancing nutritional supplement on patients at high risk of infection after cardiac surgery: A randomised placebo-controlled trial. *Lancet* **358**, 696–701 (2001).
38. U. Agarwal, I. C. Didelija, Y. Yuan, X. Wang, J. C. Marini, Supplemental citrulline is more efficient than arginine in increasing systemic arginine availability in mice. *J. Nutr.* **147**, 596–602 (2017).
39. P. C. Rodriguez, A. C. Ochoa, A. A. Al-Khami, Arginine metabolism in myeloid cells shapes innate and adaptive immunity. *Front. Immunol.* **8**, 93 (2017).
40. G. K. Grimble, Adverse gastrointestinal effects of arginine and related amino acids. *J. Nutr.* **137**, 1693S–1701S (2007).
41. C. Moinard *et al.*, Dose-ranging effects of citrulline administration on plasma amino acids and hormonal patterns in healthy subjects: The Citrudose pharmacokinetic study. *Br. J. Nutr.* **99**, 855–862 (2008).
42. R. W. M. Kempkes, I. Joosten, H. J. P. M. Koenen, X. He, Metabolic pathways involved in regulatory T cell functionality. *Front. Immunol.* **10**, 2839 (2019).
43. S. P. Cobbold *et al.*, Infectious tolerance via the consumption of essential amino acids and mTOR signaling. *Proc. Natl. Acad. Sci. U.S.A.* **106**, 12055–12060 (2009).
44. C. R. Lee *et al.*, Myeloid-derived suppressor cells are controlled by regulatory T cells via TGF-β during murine colitis. *Cell Rep.* **17**, 3219–3232 (2016).
45. F. Venet *et al.*, Lymphocytes in the development of lung inflammation: A role for regulatory CD4+ T cells in indirect pulmonary lung injury. *J. Immunol.* **183**, 3472–3480 (2009).
46. L. B. Ware *et al.*, Low plasma citrulline levels are associated with acute respiratory distress syndrome in patients with severe sepsis. *Crit. Care* **17**, R10 (2013).
47. B. Zingarelli *et al.*, Part I: Minimum quality threshold in pre-clinical sepsis studies (MQTiPSS) for study design and humane modeling endpoints. *Shock* **51**, 10–22 (2018).
48. C. Libert *et al.*, Part II: Minimum quality threshold in pre-clinical sepsis studies (MQTiPSS) for Types of infections and organ dysfunction endpoints. *Shock* **51**, 23–32 (2018).
49. J. Hellman *et al.*, Part III: Minimum quality threshold in pre-clinical sepsis studies (MQTiPSS) for fluid resuscitation and antimicrobial therapy endpoints. *Shock* **51**, 33–43 (2018).
50. M. Grégoire *et al.*, Frontline Science: HMGB1 induces neutrophil dysfunction in experimental sepsis and in patients who survive septic shock. *J. Leukoc. Biol.* **101**, 1281–1287 (2017).
51. O. Huet *et al.*, Ensuring animal welfare while meeting scientific aims using a murine pneumonia model of septic shock. *Shock* **39**, 488–494 (2013).
52. G. Matute-Bello *et al.*; Acute Lung Injury in Animals Study Group, An official American Thoracic Society workshop report: Features and measurements of experimental acute lung injury in animals. *Am. J. Respir. Cell Mol. Biol.* **44**, 725–738 (2011).
53. J. Chastre, J. Y. Fagon, Ventilator-associated pneumonia. *Am. J. Respir. Crit. Care Med.* **165**, 867–903 (2002).
54. J. M. Tadie *et al.*, HMGB1 promotes neutrophil extracellular trap formation through interactions with Toll-like receptor 4. *Am. J. Physiol. Lung Cell. Mol. Physiol.* **304**, L342–L349 (2013).

IMMUNOLOGY AND INFLAMMATION

Reizine et al.
Beneficial effects of citrulline enteral administration on sepsis-induced T cell mitochondrial dysfunction

PNAS | 9 of 9
https://doi.org/10.1073/pnas.2115139119